Biochemical and Biophysical Research Communications 446 (2014) 370–374

Contents lists available at ScienceDirect

Biochemical and Biophysical Research Communications

journal homepage: www.elsevier.com/locate/ybbrc

Mechanism of tetrodotoxin block and resistance in sodium channels

Rong Chen *, Shin-Ho Chung

Research School of Biology, Australian National University, Canberra ACT 0200, Australia

ARTICLE INFO

Article history:
Received 23 February 2014
Available online 4 March 2014

Keywords:
Sodium channel
Na_VAb
Ion channel block
Hydrogen bond network
Molecular dynamics

ABSTRACT

Tetrodotoxin (TTX) has been used for many decades to characterize the structure and function of biological ion channels. Yet, the precise mechanism by which TTX blocks voltage-gated sodium (Na_V) channels is not fully understood. Here molecular dynamics simulations are used to elucidate how TTX blocks mammalian voltage-gated sodium (Nav) channels and why it fails to be effective for the bacterial sodium channel, Na_VAb. We find that, in Na_VAb, a sodium ion competes with TTX for the binding site at the extracellular end of the filter, thus reducing the blocking efficacy of TTX. Using a model of the skeletal muscle channel, $Na_V1.4$, we show that the conduction properties of the channel observed experimentally are faithfully reproduced. We find that TTX occludes the entrance of $Na_V1.4$ by forming a network of hydrogen-bonds at the outer lumen of the selectivity filter. The guanidine group of TTX adopts a lateral orientation, rather than pointing into the filter as proposed previously. The acidic residues just above the selectivity filter are important in stabilizing the hydrogen-bond network between TTX and $Na_V1.4$. The effect of two single mutations of a critical tyrosine residue in the filter of $Na_V1.4$ on TTX binding observed experimentally is reproduced using computational mutagenesis.

1. Introduction

Tetrodotoxin (TTX) is a guanidinium compound produced by bacteria in puffer fish and certain other animals such as octopus and chaetognatha. Due to its potent inhibitory effect on several isoforms of voltage-gated Na^+ (Na_V) channels, TTX has been extensively studied in biological and chemical sciences [1]. TTX also has promising pharmacological applications, such as the treatment of severe pain in cancer patients [2].

TTX, the molecular formula of which is $C_{11}H_{17}N_3O_8$ (see molecular structure in Fig. S1 of the Supplementary Material), inhibits certain Na_V channel isoforms such as the skeletal muscle channel, $Na_V1.4$, at nanomolar concentrations by physically occluding the ion conduction pathway [3]. Several residues inside and just outside the filter have been shown to be particularly important for TTX inhibition [4,5]. According to the molecular models proposed previously [6,7], the guanidine group of TTX protrudes into the narrow filter, where it interacts favorably with the two acidic residues of the characteristic DEKA ring at position 177 (Fig. S1B). Although these models are consistent with the pore-blocking mechanism of TTX, they have difficulties in explaining some of the experimental data available. For example, these models would predict that introducing more negative charged residues to the filter would increase the affinity of TTX. However, this is not seen experimentally; the mutation of the alanine of the DEKA king to a glutamate actually reduces the affinity of TTX by about 50 fold without affecting the conductance of the channel significantly [8]. The bacterial Na_V channels NaChBac and Na_VAb, in which the DEKA ring (net charge $-1\ e$) is replaced by an EEEE ring (net charge $-4\ e$), are insensitive to TTX even at micromolar toxin concentrations [9]. In fact, experimental evidence has pointed to the importance of the outer charged ring (positions 180 and 181, Fig. S1B) in TTX block of Na_V channels [5,8]. Thus, the guanidine group of TTX may interact with the outer charged ring more intimately, rather than protruding into the filter.

Here the inhibition of Na_VAb and $Na_V1.4$ by TTX is examined in atomic detail using molecular dynamics (MD) simulations. We show that the TTX-resistance of Na_VAb is accounted for by the inability of TTX guanidine to form strong interactions with the channel in the presence of two Na^+ ions in the filter. On the other hand, the outer charged ring of $Na_V1.4$ is able to form a hydrogen-bond (H-bond) network with TTX. The guanidine group of TTX adopts a lateral orientation relative to the filter on blocking $Na_V1.4$, in contrast to an inward orientation proposed in previous models [6,7].

Abbreviations: MD, molecular dynamics; Na_V, voltage-gated sodium; PMF, potential of mean force; TTX, tetrodotoxin.

* Corresponding author. Fax: +61 2 6125 0739.
E-mail address: rong.chen@anu.edu.au (R. Chen).

http://dx.doi.org/10.1016/j.bbrc.2014.02.115
0006-291X/

2. Methods

2.1. Molecular dynamics

The equilibrated structure of Na_VAb embedded in a lipid bilayer and a box of explicit water is taken from our previous study [10]. A model of $Na_V1.4$ is constructed based on the crystal structure of Na_VAb (See Supplementary Material for details). In all simulation boxes the concentration of NaCl is 0.2 M. All MD simulations are performed under periodic boundary conditions using NAMD 2.9 [11]. The CHARMM36 force fields for lipids and proteins and the TIP3P model for water are used. The CHARMM general force field [12] is used to describe TTX. The topology and atomic charges of TTX are generated using the ParamChem server (https://www.paramchem.org) [13,14]. The penalty score is less than 50 for 90% of atoms and less than 10 for ~50% of atoms, indicating that the analogy of TTX with existing molecules in the force field is reasonable. The switch and cutoff distances for short-range interactions are set to 8.0 and 12.0 Å, respectively. The long-range electrostatic interactions are accounted for using the particle mesh Ewald method, with a maximum grid spacing of 1.0 Å. Bond lengths are maintained rigid with the SHAKE and SETTLE algorithms. A time step of 2 fs is used. The temperature and pressure are maintained constant at 300 K on average by using the Langevin dynamics (damping coefficient 1 ps^{-1}), and an average of 1 atm by using Nosé–Hoover Langevin Piston method, respectively. The barostat oscillation and damping time scale are set to 200 and 100 ps, respectively. The pressure coupling is semiisotropic. Trajectories are saved every 20 ps for analysis. The potential of mean force (PMF) profiles for the binding of TTX to Na_VAb and $Na_V1.4$ are constructed using the umbrella sampling method. Details of the umbrella sampling calculations are given in the Supplementary Material.

2.2. Brownian dynamics

To validate our model of $Na_V1.4$ the conductance properties of the channel are deduced using three-dimensional Brownian dynamics simulations [15]. In these simulations, 14 Na^+ and 14 Cl^- ions are placed in each of the two cylindrical reservoirs of 30 Å in radius connected to the channel. The ion concentration is 0.14 M in both reservoirs. The position and velocity of each ion evolves according to a stochastic dynamical system. The electrostatic forces experienced by the ions are derived from pre-calculated lookup tables containing the solutions to Poisson's equation [16]. The adaptive Poisson–Boltzmann Solver [17] is used to derive the electric field generated by the partial charges in the channel protein. A time step of 100 fs is used in the reservoirs and 2 fs in the channel. Each simulation is run for 10 μs. The current is computed from the number of ions that pass through an imaginary plane near the end of the channel during a simulation period.

3. Results

3.1. Binding to Na_VAb

To probe the most favorable position of TTX relative to the filter of Na_VAb and deduce the mechanism of TTX resistance by Na_VAb, we place TTX near the extracellular end of the filter of Na_VAb, with the guanidine group of TTX pointing into the filter. Two different systems, in which the selectivity filter contains one and two Na^+ ions, respectively, are considered. The systems are simulated for 20 ns each without restraints. In both simulations the guanidine group of TTX remains imbedded into the filter after 20 ns (Fig. 1). The guanidine group of TTX is closely coupled with the characteristic EEEE ring at position 177 in the selectivity filter of the channel (Fig. 1A). In the case of one filter ion, TTX forms strong electrostatic interactions with the EEEE ring in the filter, while the electrostatic interactions between TTX and the EEEE ring are significantly weaker in the case of two filter ions. The difference in the electrostatic interaction energy between TTX and Na_VAb is about 3-fold depending on the ion configuration of the filter, which is reflected in the PMF profiles of TTX binding in the two systems (Fig. 2A). The PMF profile in the presence of one filter ion has a depth of 17 kT, corresponding to a K_d value of 575 nM. In contrast, the profile in the presence of two filter ions has a depth of only 5 kT, corresponding to a K_d value of 60 mM. Thus, the presence of a second Na^+ ion in the filter causes the binding affinity of TTX-$Na_V1.4$ to reduce by five orders of magnitude. Previous computational studies have revealed that in the absence of a membrane potential two or three Na^+ ions would occupy the filter of Na_VAb in the pre-open state [18,19]. Our calculations predict that Na_VAb, whose filter is predominantly occupied by two ions, is resistant to TTX, consistent with the experimental results of Ren et al. [9].

3.2. Conduction properties of $Na_V1.4$

We use Brownian dynamics to ascertain whether our model of $Na_V1.4$ can faithfully reproduce the conduction properties of the channel. Using the initial model we constructed, the channel is found to conduct Na^+ ions inwardly but not outwardly. This rectification is due to the truncation of negatively-charged residues near the intracellular gate. These negative charges attract permeating ions from the reservoir to the gate. Extending the S6 helix by 15 residues eliminates the rectification without affecting the inward conductance of the channel significantly. The current–voltage curve of the modified channel model, as determined from Brownian dynamics (Fig. S2), is linear and shows no rectification in accord

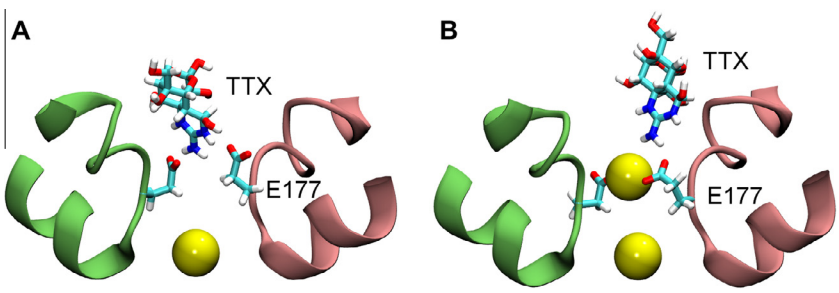

Fig. 1. TTX bound to the filter of Na_VAb in the presence of one (A) and two (B) Na^+ ions (yellow spheres) in the filter. The backbones of two channel subunits are shown as pink and lime ribbons. The side chains of Glu177 from the two subunits are shown. The view is perpendicular to the channel axis. (For interpretation of the references to color in this figure legend, the reader is referred to the web version of this article.)

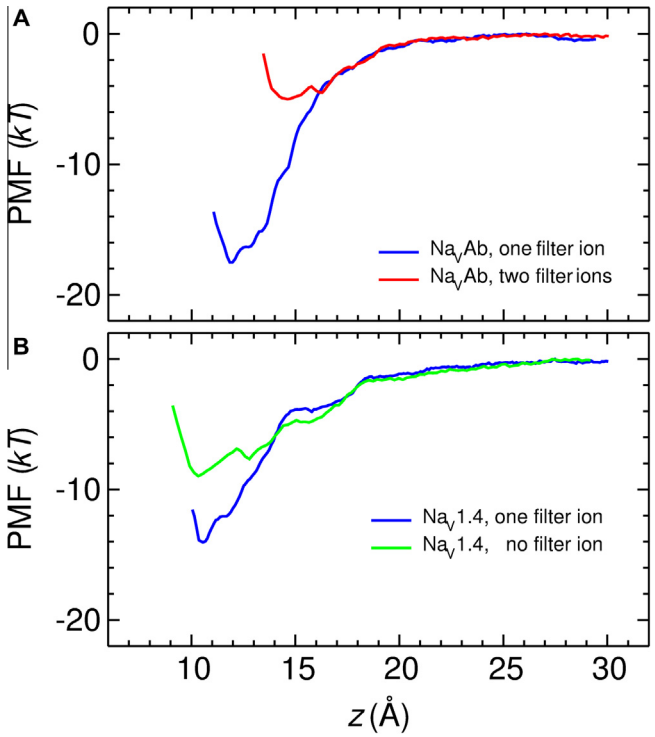

Fig. 2. PMF profiles for the binding of TTX to Na_VAb (A) and $Na_V1.4$ (B). The reaction coordinate, *z*, is the distance between TTX and the channel backbone atoms along the channel axis.

with experiment [20]. The conductance of the $Na_V1.4$ model is calculated to be 50–70 pS, within 3 fold to the experimental value of 25 pS [21].

3.3. Binding to $Na_V1.4$

To understand the high-affinity binding of TTX to $Na_V1.4$, we examine how TTX would bind to the selectivity filter of $Na_V1.4$. In contrast to Na_VAb which is a homo-tetramer, $Na_V1.4$ is an integral protein consisting of four homologous but non-identical domains (DI, DII, DIII and DIV). TTX is placed at the extracellular lumen of the filter, with the guanidine group of TTX pointing into the filter. The system is simulated extensively for 50 ns without restraints.

During the first 10 ns of the equilibrium simulation, TTX moves out of the filter rapidly, with its long axis becoming perpendicular to the channel axis (Fig. S3). Then TTX moves back into the filter, while its long axis remains perpendicular to the channel axis at 20 ns. Afterwards the position and orientation of TTX remains stable until the simulation is terminated at 50 ns (Fig. S3).

During the last 30 ns, TTX fully occludes outer entrance of the filter of $Na_V1.4$ (Fig. 3A), forming six H-bonds with acidic residues from the channel (Fig. 3B). The guanidine group and two hydroxyl groups (positions 4 and 11) of TTX, and three acidic residues just outside the filter of the channel are involved in the formation of the H-bond network (Fig. 3B). In addition, the hydroxyl group at position 9 forms a transient H-bond with the side chain of Glu177 inside the filter (Fig. 3C). The H-bond network stabilizes the binding of TTX to $Na_V1.4$, rendering the high-affinity inhibition of $Na_V1.4$ by TTX. The Tyr178 (DI) residue of the filter, which is important for TTX specificity [5,22], is in close contact with TTX (Fig. 3D).

Residue Asp181 (DIII) of $Na_V1.4$ forms two H-bonds with the guanidine group of TTX in the bound complex at equilibrium (Fig. 3B). In the absence of TTX, a Na^+ ion is observed to be in contact with DIII-Asp181 (Fig. S4). This binding site closely resembles that observed in the crystal structure of a bacterial sodium channel, which is believed to be common to mammalian Na_V channels [23]. Thus, the TTX-$Na_V1.4$ complex we constructed predicts that

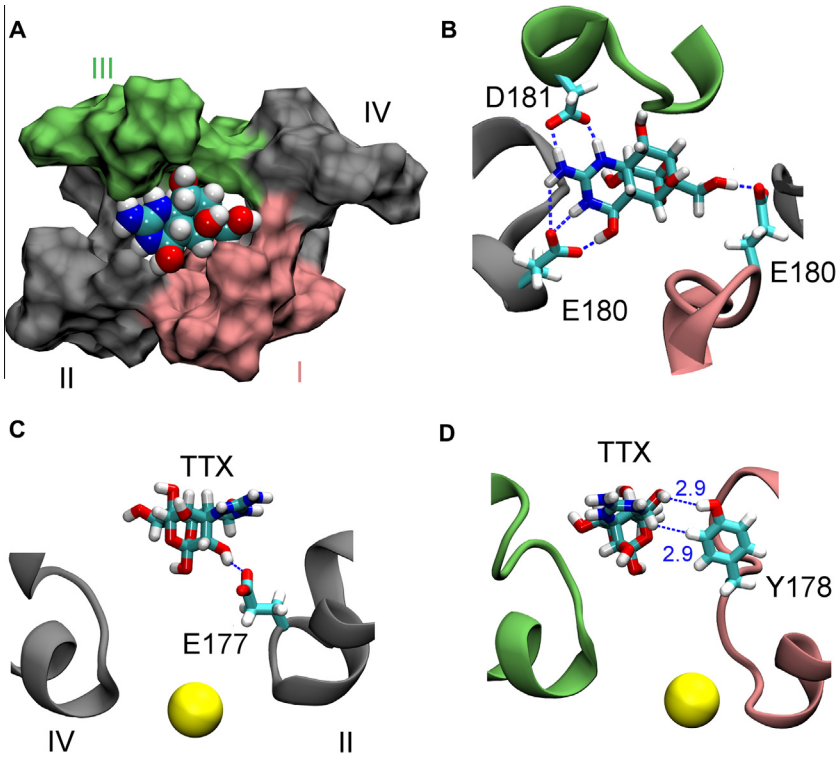

Fig. 3. Position of TTX relative to the filter of $Na_V1.4$ after 50 ns of an unbiased MD simulation. In (B) and (C), the H-bonds between TTX and four acidic residues from the channel are indicated (blue dashed lines). In (D), the numbers represent the inter-atomic distances in angstroms. Yellow spheres represent the Na^+ ion in the filter. (For interpretation of the references to color in this figure legend, the reader is referred to the web version of this article.)

the binding sites of TTX and a Na^+ ion overlap at the outer lumen of the filter, consistent with the trapped-ion mechanism [24]. The affinity of TTX would be lower if a Na^+ ion has a higher propensity to be bound to DIII-Asp181.

3.4. Ion occupancy in filter

TTX block can be enhanced significantly by repetitive depolarization [24]. This use-dependent block of TTX may be attributed to changes in either ion occupancy or conformation of the filter during depolarization [25]. To ascertain the effect of the Na^+ ion at the inner end of the filter on TTX binding, we move the ion from the filter to the bulk and equilibrate the TTX-Na_V1.4 complex using unbiased MD. The position of TTX relative to the filter of Na_V1.4 does not evolve significantly after 20 ns and the channel remains to be fully blocked by TTX. However, PMF calculations show that the binding affinity of TTX is significantly weakened due to the absence of the Na^+ ion (Fig. 2B). The weakening of TTX binding is unlikely due to electrostatic interactions between TTX and the ion; otherwise TTX binding should be strengthened in the absence of the ion. Rather, TTX only forms four H-bonds with the channel, as opposed to six H-bonds in the presence of one filter ion. Thus, the absence of the filter ion induces small conformational changes to the filter, such that the H-bond network between TTX and the channel is interrupted. Our interpretation is consistent with Huang et al. [25], who suggested that depolarization-induced conformational changes to the filter are involved in the use-dependence of TTX block.

3.5. Computational mutagenesis

To validate our model of TTX-Na_V1.4, we carry out computational mutagenesis simulations and compare our predictions to that determined experimentally. Specifically, two single mutations (Y178D and Y178C) to the channel are considered; these two mutations have been shown experimentally to reduce the affinity of TTX by three orders of magnitude and largely account for the resistance of several Na_V channel isoforms to TTX [5]. The effect of the two mutations on the binding affinity of TTX observed experimentally is reproduced.

In the bound complex of TTX-Na_V1.4, Tyr178 from DI is within 3 Å of TTX (Fig. 3D). We replace this tyrosine with an aspartate or cysteine, and subsequently equilibrate each system for 10 ns without restraints. The position of TTX relative to the filter is not observed to change appreciably for both mutants (Fig. S5). However, the residue at position 178 of subunit I in the mutant channels is no longer in direct contact with TTX (Fig. S5). This observation is consistent with the binding affinity of TTX being significantly reduced by the mutations. The PMF profile for the wild type Na_V1.4 is ~5 kT deeper than that of the two mutant channels (Fig. S6), corresponding to an approximately 150 fold reduction in the K_d value. The contact area between TTX and the channel is significantly reduced by the mutations (WT, 256 $Å^2$; Y178C, 237 $Å^2$; Y178D, 241 $Å^2$; standard error is <1 $Å^2$ in all cases). In addition, the average number of H-bonds is reduced from six for the WT to four (Y178D) or five (Y178C) for the mutant channels. Thus, without the support from the bulky tyrosine residue at position 178, the H-bond network between TTX and Na_V1.4 is weakened, resulting in TTX-resistance in the mutant Na_V1.4 channels. The affinity changes resulting from Y178D and Y178C mutations observed experimentally are reproduced with our TTX-Na_V1.4 model.

Our model of TTX-Na_V1.4 is also consistent with some other mutagenesis data available. For example, Glu180 forms three H-bonds with TTX which are critical for the formation of the H-bond network (Fig. 3B). Any mutation of Glu180 could disrupt the H-bond network, thereby weakening TTX binding. Indeed, the mutation of Glu180 to an aspartate reduces the affinity of TTX by three orders of magnitude [26]. We note, however, that conformational changes of the filter, which have been demonstrated experimentally for several mutant channels [8], should be considered in the interpretation of mutagenesis data.

4. Discussion

The complex structures formed between TTX and two voltage-activated sodium channels, Na_VAb and Na_V1.4, are examined in atomic detail to understand how the toxin binds to the external vestibule of the channels. We show that the resistance of Na_VAb to TTX block observed experimentally is due to two Na^+ ions being trapped in the channel filter. On the other hand, TTX firmly blocks Na_V1.4 by forming an H-bond network with three acidic residues just outside the filter. To form this H-bond network, the guanidine group of TTX must adopt a lateral orientation, as opposed to protruding into the filter as previously thought.

Two key differences in the filter of Na_VAb and Na_V1.4 render the different sensitivity of these two channels to TTX block. The inner charged ring of Na_VAb (EEEE ring) is more negatively charged than that of Na_V1.4 (DEKA ring). As such the Na_VAb filter has a higher propensity for Na^+ ions, which compete with TTX for binding, resulting in TTX-resistance. On the other hand, Na_V1.4 carries an outer charged ring which is not present in Na_VAb. The outer charged ring forms a network of hydrogen bonds with TTX, and therefore renders the channel TTX-sensitive.

The H-bond network of TTX-Na_V1.4 shown here can be used to interpret the affinities of several TTX analogues for Na_V1.4 observed experimentally. For example, removing the hydroxyl group from C9 and C11 of TTX has been found to reduce the affinity of TTX by two orders of magnitude [27]. In our TTX-Na_V1.4 complex (Fig. 3), the hydroxyl groups connected to C9 and C11 are involved in the formation of the H-bond network. Without these hydroxyl groups the H-bond network would be perturbed and the binding weakened.

Acknowledgments

This research was undertaken on the National Computational Infrastructure in Canberra, Australia, which is supported by the Australian Commonwealth Government. This work was supported by the National Health and Medical Research Council (NHMRC) of Australia and The Medical Advances Without Animals Trust (MAWA). We thank Dr. Anna Robinson for assistance in homology modeling of Na_V1.4.

Appendix A. Supplementary data

Supplementary data associated with this article can be found, in the online version, at http://dx.doi.org/10.1016/j.bbrc.2014.02.115.

References

[1] E.G. Moczydlowski, The molecular mystique of tetrodotoxin, Toxicon 63 (2013) 165–183.
[2] N.A. Hagen, B. Lapointe, M. Ong-Lam, B. Dubuc, D. Walde, B. Gagnon, R. Love, R. Goel, P. Hawley, A.H. Ngoc, P. du Souich, A multicentre open-label safety and efficacy study of tetrodotoxin for cancer pain, Curr. Oncol. 18 (2011) e109–e116.
[3] R.J. French, D. Yoshikami, M.F. Sheets, B.M. Olivera, The tetrodotoxin receptor of voltage-gated sodium channels – perspectives from interactions with μ-conotoxins, Mar. Drugs 8 (2010) 2153–2161.
[4] G. Choudhary, M. Yotsu-Yamashita, L. Shang, T. Yasumoto, S.C. Dudley Jr., Interactions of the C-11 hydroxyl of tetrodotoxin with the sodium channel outer vestibule, Biophys. J. 84 (2003) 287–294.
[5] J.L. Penzotti, H.A. Fozzard, G.M. Lipkind, S.C. Dudley, Differences in saxitoxin and tetrodotoxin binding revealed by mutagenesis of the Na^+ channel outer vestibule, Biophys. J. 75 (1998) 2647–2657.

[6] G.M. Lipkind, H.A. Fozzard, A structural model of the tetrodotoxin and saxitoxin binding site of the Na^+ channel, Biophys. J. 66 (1994) 1–13.
[7] D.B. Tikhonov, B.S. Zhorov, Architecture and pore block of eukaryotic voltage-gated sodium channels in view of Na_VAb bacterial sodium channel structure, Mol. Pharmacol. 82 (2012) 97–104.
[8] H. Terlau, S.H. Heinemann, W. Stuhmer, M. Pusch, F. Conti, K. Imoto, S. Numa, Mapping the site of block by tetrodotoxin and saxitoxin of sodium channel II, FEBS Lett. 293 (1991) 93–96.
[9] D. Ren, B. Navarro, H. Xu, L. Yue, Q. Shi, D.E. Clapham, A prokaryotic voltage-gated sodium channel, Science 294 (2001) 2372–2375.
[10] R. Chen, S.H. Chung, Binding modes of μ-conotoxin to the bacterial sodium channel (Na_VAb), Biophys. J. 102 (2012) 483–488.
[11] J.C. Phillips, R. Braun, W. Wang, J. Gumbart, E. Tajkhorshid, E. Villa, C. Chipot, R.D. Skeel, L. Kalé, K. Schulten, Scalable molecular dynamics with NAMD, J. Comput. Chem. 26 (2005) 1781–1802.
[12] K. Vanommeslaeghe, E. Hatcher, C. Acharya, S. Kundu, S. Zhong, J. Shim, E. Darian, O. Guvench, P. Lopes, I. Vorobyov, A.D. Mackerell Jr., CHARMM general force field: a force field for drug-like molecules compatible with the CHARMM all-atom additive biological force fields, J. Comput. Chem. 31 (2010) 671–690.
[13] K. Vanommeslaeghe, A.D. MacKerell Jr., Automation of the CHARMM General Force Field (CGenFF) I: bond perception and atom typing, J. Chem. Inf. Model. 52 (2012) 3144–3154.
[14] K. Vanommeslaeghe, E.P. Raman, A.D. MacKerell Jr., Automation of the CHARMM General Force Field (CGenFF) II: assignment of bonded parameters and partial atomic charges, J. Chem. Inf. Model. 52 (2012) 3155–3168.
[15] S.H. Chung, T.W. Allen, S. Kuyucak, Modeling diverse range of potassium channels with Brownian dynamics, Biophys. J. 83 (2002) 263–277.
[16] M. Hoyles, S. Kuyucak, S.H. Chung, Solutions of Poisson's equation in channel-like geometries, Comput. Phys. Commun. 115 (1998) 45–68.
[17] N.A. Baker, D. Sept, S. Joseph, M.J. Holst, J.A. McCammon, Electrostatics of nanosystems: application to microtubules and the ribosome, Proc. Natl. Acad. Sci. USA 98 (2001) 10037–10041.
[18] N. Chakrabarti, C. Ing, J. Payandeh, N. Zheng, W.A. Catterall, R. Pomès, Catalysis of Na^+ permeation in the bacterial sodium channel Na_VAb, Proc. Natl. Acad. Sci. USA 110 (2013) 11331–11336.
[19] V. Carnevale, W. Treptow, M.L. Klein, Sodium ion binding sites and hydration in the lumen of a bacterial ion channel from molecular dynamics simulations, J. Phys. Chem. Lett. 2 (2011) 2504–2508.
[20] M. Chahine, P.B. Bennett, A.L. George Jr., R. Horn, Functional expression and properties of the human skeletal muscle sodium channel, Pflügers Arch. 427 (1994) 136–142.
[21] W.A. Catterall, A.L. Goldin, S.G. Waxman, International Union of Pharmacology. XLVII. Nomenclature and structure–function relationships of voltage-gated sodium channels, Pharmacol. Rev. 57 (2005) 397–409.
[22] H.A. Fozzard, G.M. Lipkind, The tetrodotoxin binding site is within the outer vestibule of the sodium channel, Mar. Drugs 8 (2010) 219–234.
[23] D. Shaya, F. Findeisen, F. Abderemane-Ali, C. Arrigoni, S. Wong, S.R. Nurva, G. Loussouarn, D.L. Minor Jr., Structure of a prokaryotic sodium channel pore reveals essential gating elements and an outer ion binding site common to eukaryotic channels, J. Mol. Biol. 426 (2014) 467–483.
[24] F. Conti, A. Gheri, M. Pusch, O. Moran, Use dependence of tetrodotoxin block of sodium channels: a revival of the trapped-ion mechanism, Biophys. J. 71 (1996) 1295–1312.
[25] C.J. Huang, L. Schild, E.G. Moczydlowski, Use-dependent block of the voltage-gated Na^+ channel by tetrodotoxin and saxitoxin: effect of pore mutations that change ionic selectivity, J. Gen. Physiol. 140 (2012) 435–454.
[26] K.J. Kontis, A.L. Goldin, Site-directed mutagenesis of the putative pore region of the rat IIA sodium channel, Mol. Pharmacol. 43 (1993) 635–644.
[27] C. Rosker, B. Lohberger, D. Hofer, B. Steinecker, S. Quasthoff, W. Schreibmayer, The TTX metabolite 4,9-anhydro-TTX is a highly specific blocker of the $Na_V1.6$ voltage-dependent sodium channel, Am. J. Physiol. 293 (2007) C783–C789.